Polycyclic aromatic hydrocarbons for organic photovoltaics

Wallace W. H. Wong*
School of Chemistry, Bio21 Institute, University of Melbourne, 30 Flemington Road, Parkville, Victoria 3010, Australia

ABSTRACT

Hexa-*peri*-hexabenzocoronene (HBC) is a disc-shaped polycyclic aromatic hydrocarbon with remarkable self-association properties. Solution processable alkyl substituted HBC compounds often exhibit discotic liquid crystalline behavior and have been shown to carry charges efficiently in bulk. In recent years, fluorenyl HBC (FHBC) compounds have emerged as promising materials for organic photovoltaics. The fluorene substituent imparts solution processability while maintaining good charge transport characteristics. Power conversion efficiency close to 3% has been reported for organic solar cell devices containing FHBC materials.

Keywords: hexabenzocoronene, self-assembly, charge mobility, organic photovoltaics, organic solar cells

1. INTRODUCTION

Polycyclic aromatic hydrocarbons (PAH) are a family of planar conjugated materials that can be considered as small discrete sections of a graphene sheet.[1, 2] From linear acenes to disc-shape pyrenes and coronenes, the photophysical properties of PAHs are not only defined by the numbers of fused rings or degree of conjugation and the shape of the molecule but also intermolecular interactions driven by their highly delocalized π system. Their strong intermolecular association also leads to interesting bulk material properties such as crystallinity and charge transport.[1] It is their bulk properties that make PAHs particularly interesting materials for organic electronic applications.[2]

Hexa-*peri*-hexabenzocoronene (HBC) is a disc-shape PAH consisting of 13 six-membered rings.[3] HBC and its derivatives have been shown to self-assemble into columnar structures and discotic liquid crystalline behavior has been observed in many cases.[4] As a result of the strong self-association, HBC is a difficult compound to process if solubilising side chains are not incorporated. By controlling the structure of the solubilising groups, a variety of liquid crystals,[5] organogels[6] and nanotubes[7, 8] can be obtained through self-assembly. While flexible alkyl or alkoxy side chains have been used extensively on the periphery of the HBC molecule, rigid aromatic functional groups are relatively rare. Recently, a new class of 9,9-dioctylfluorene functionalized HBC (FHBC) materials has been developed in our group.[9-11] The fluorene unit not only imparts solubility on the HBC core but also enables facile extension. This new strategy has led to a range of hybrid compounds incorporating thiophene[12] and porphyrin[13] chromophores as well as electroactive fullerenes.[14] In this article, we will summarize our work on FHBC derivatives and discuss insights gained particularly for organic photovoltaic applications.

2. SYNTHESIS AND MOLECULAR PROPERTIES

Synthesis of HBC derivatives is well-known in the literature.[2] Following the early work by Clar,[15] a number of research groups, particularly the group of Müllen, have expanded the range of possible functional groups on the HBC molecule.[1, 2] A variety of regio-substitution patterns is also available including hexakis- and bis-substituted products (Scheme 1). The hexakis-substituted FHBC **1** was synthesized starting from the cobalt-catalyzed trimerization of diphenylacetylene **4**.[11] Bromination of hexaphenylbenzene **5** followed by Suzuki-Miyaura coupling with the 9,9-dioctylfluorene boronic acid pinacol ester derivative **7** gave the fluorene functionalized hexaphenylbenzene **8** (Scheme 1). Displacement of the trimethylsilyl group with halide was followed by the key step involving the conversion of the hexaphenylbenzene derivative to FHBC **9** via oxidative cyclodehydrogenation. FHBC **9** can be readily converted to FHBC **1** by removal of the halide substituent or can be further derivatized (Scheme 1).[10]

* wwhwong@unimelb.edu.au

2,5-Bis(9,9-dioctylfluorenyl)hexa-*peri*-hexabenzocoronene **2** was synthesized via the cyclopentadienone intermediate **13** (Scheme 1).[11] Diels-Alder addition of diphenylacetylene **12** to **13** followed by CO extrusion gave hexaphenylbenzene derivative **14** (Scheme 1). Iodination, oxidative dehydrogenation followed by halide removal led to 2,5-bis-substituted FHBC **2**. The 2,11-bis-substituted FHBC **3** was synthesized through a similar sequence of reactions (Scheme 1). The iodo-functionalized FHBC compounds **9**, **15** and **21** can be readily derivatized by transition metal catalysed coupling reactions. Scheme 2 illustrates a range of functional groups that has been attached to the 2,11-bis-substituted FHBC core.

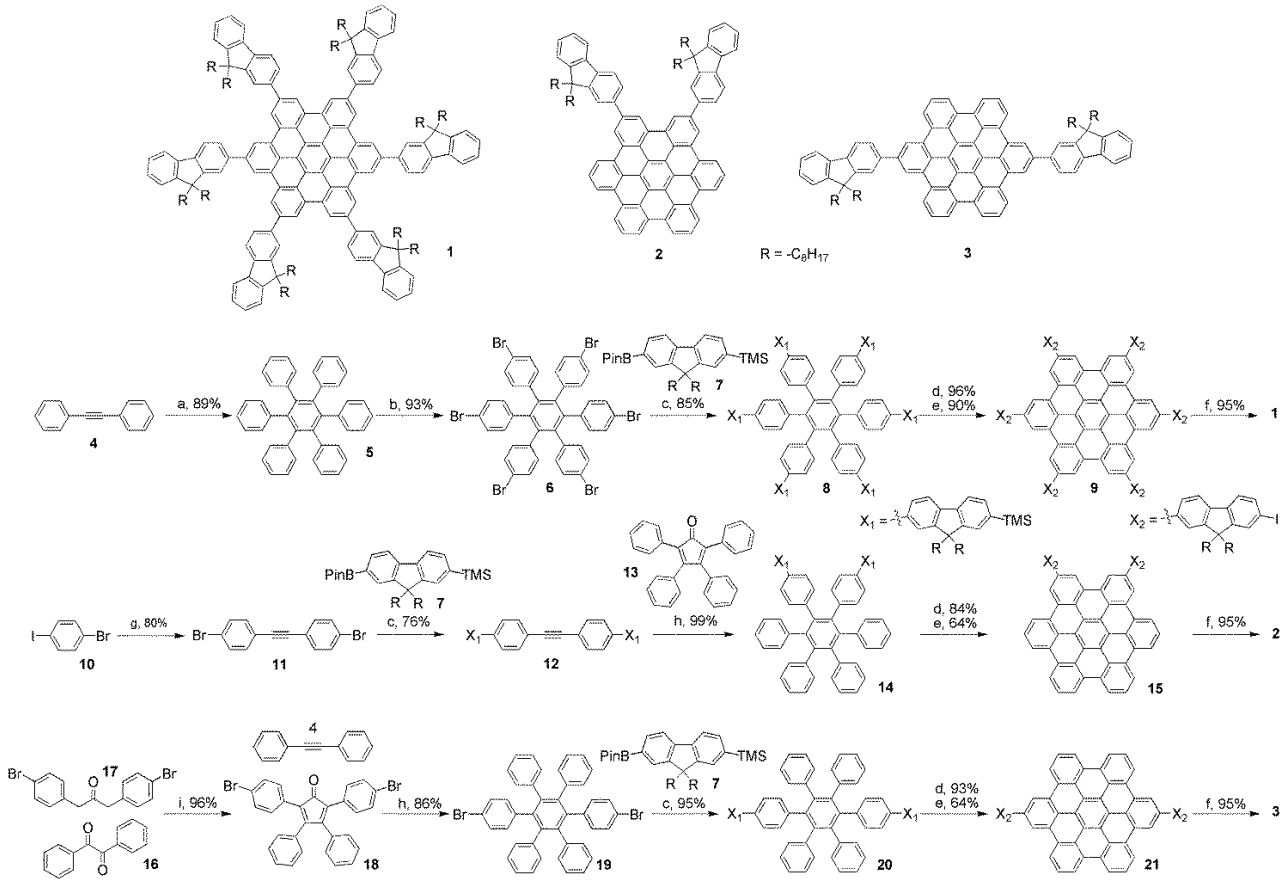

Scheme 1. Synthesis of FHBC **1**, **2** and **3**. a) $Co_2(CO)_8$, 1,4-dioxane, 100 °C, 24 h; b) Br_2, -20 to 25 °C; c) $Pd(PPh_3)_4$, Et_4NOH (aq.), toluene, 90 °C; d) ICl (1 M in CH_2Cl_2), 0 to 25 °C; e) $FeCl_3$ in CH_3NO_2, CH_2Cl_2, N_2 bubbling, 25 °C, 1 h; f) nBuLi, THF, -78 °C, H_2O, -78 to 25 °C; g) $Pd(PPh_3)_2Cl_2$, CuI, DBU, trimethylsilylacetylene, THF, 60 °C; h) Ph_2O, 260 °C; i) Bu_4NOH (1 M in MeOH), 1,4-dioxane, 100 °C.

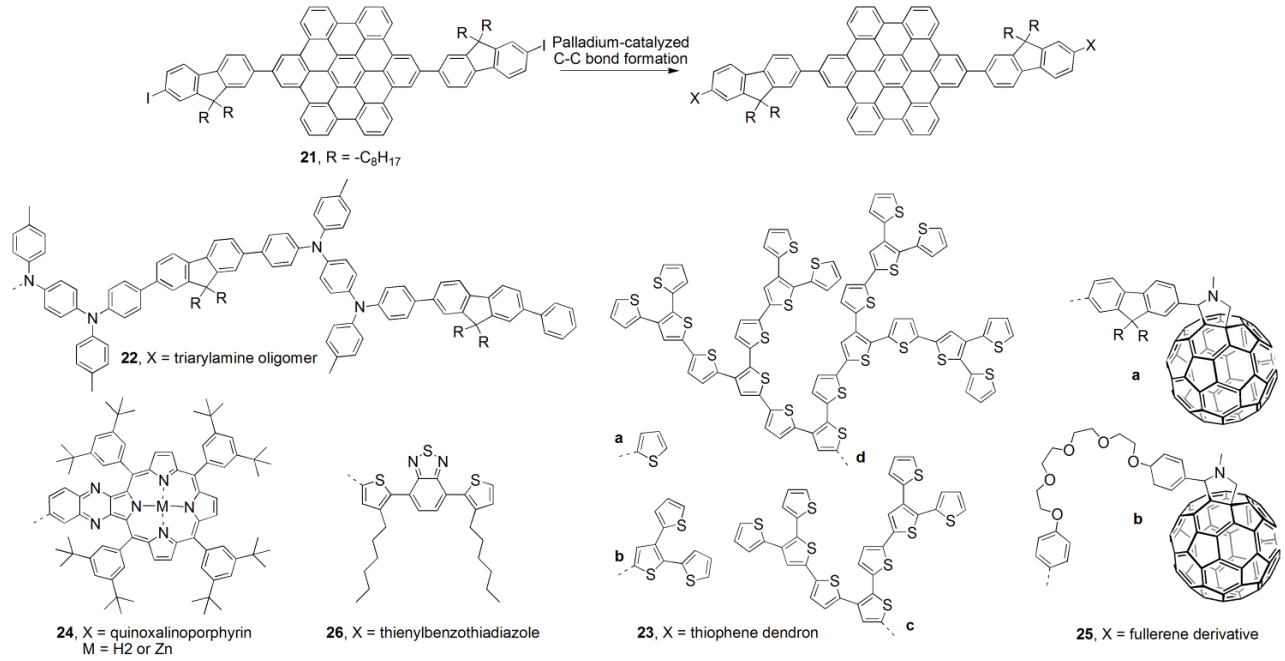

Scheme 2. Range of FHBC derivatives synthesized from 2,11-bis-substituted FHBC precursor **21**.

The UV-vis spectrum of FHBC compounds **2** and **3** is similar to that of unsubstituted HBC in trichlorobenzene as reported by Clar (Figure 1a).[16] Similar to other PAHs, HBC exhibits three characteristic electronic absorption bands namely α, p, and *β* band based on the nomenclature introduced by Clar.[15, 17] The α-band which has the longest wavelength of the three characteristic bands appears around 440 nm with low intensity and is attributed to the electronic transition from the second highest occupied molecular orbital (HOMO-1) to the lowest unoccupied molecular orbital (LUMO) also known as the 0-0 transition.[18] The p-band appears around 387 nm with moderate intensity and corresponds to a transition from HOMO to LUMO orbital.[18] The *β*-band appears around a shorter wavelength of 360 nm with high intensity due the electronic transition from the HOMO to the second lowest unoccupied orbital (LUMO+1).[18] Interestingly, the UV-vis spectrum of hexakis-substituted FHBC **1** has absorption bands at longer wavelengths (~50 nm shift) compared to bis-substituted compounds **2** and **3** (Figure 1a).[10] Upon further derivatization, the UV-vis absorption of FHBC derivatives can be broadened as illustrated by thiophene dendron-substituted FHBC compounds **23a-d** (Figure 1b).[12] However, the broadening of the spectrum is largely due to the absorption of the thiophene substituent rather than any extension in conjugation between the FHBC core and the functional group. The absorption of FHBC compounds are further broadened in solid state which is indicative of strong molecular aggregation (Figure 1b). The photoluminescence (PL) spectrum of FHBC-thiophene hybrid compounds **23a-d** are shown in Figure 1c.[12] Emission from the HBC core was observed for compounds **3**, **23a** and **23b** starting at 465 nm. For compounds **23c** and **23d**, there is clear energy transfer from the HBC core to the thiophene dendron with only emission (530 and 560 nm) from the thiophene substituent observed (Figure 1c). Similarly, efficient energy transfer was observed for the FHBC-porphyrin hybrid compound **24** (Figure 1d).[13] Emission from the FHBC core is almost completely quenched and strong emission (660 and 730 nm) from the porphyrin unit was recorded (Figure 1d). By performing electrochemical experiments, the HOMO energy level of FHBC compounds can be calculated from the oxidation data (Figure 2). By combining the electrochemical data and the optical HOMO-LUMO energy gap from absorption data, the LUMO energy levels of FHBC compounds were also obtained (Figure 2). Interestingly, the HOMO energy levels of most FHBC compounds are at around -5.3 eV. The only exception is FHBC-triarylamine compound **22** (-4.7 eV) where the HOMO level measured belonged to the triarylamine substituent (Figure 2).[11]

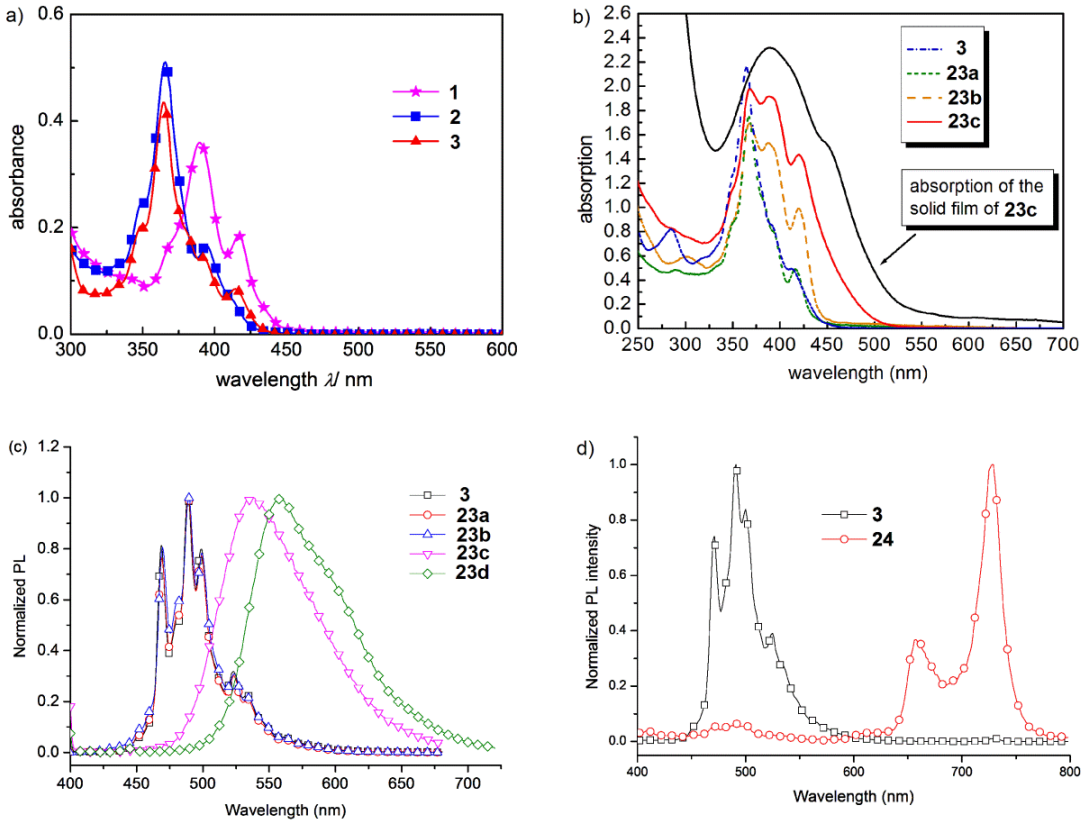

Figure 1. UV-vis and PL spectrum of FHBC derivatives.

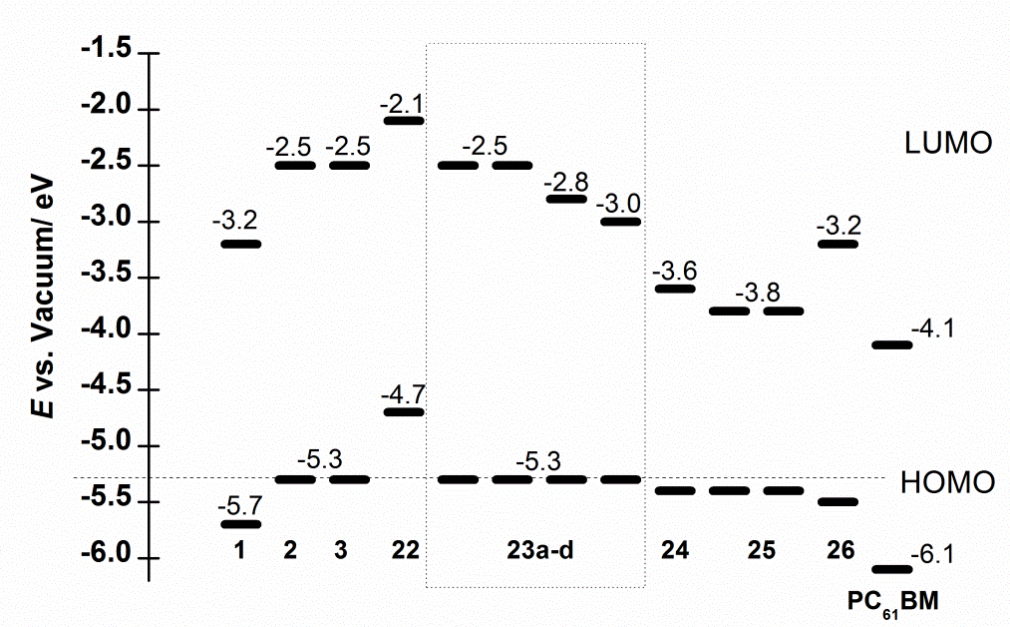

Figure 2. Energy level diagram showing the HOMO and LUMO energy levels of various FHBC derivatives.

3. SELF-ASSEMBLY AND BULK PROPERTIES

The planar aromatic nature of HBC compounds drives strong π–π intermolecular association. This is usually observed in both solution and in solid state. FHBC compounds **2** and **3** also showed strong aggregation despite the bulky fluorene units.[10] Figure 3 shows the ^{1}H NMR spectrum of compounds **2** and **3** at various solution concentrations. There are significant up field shifts in the spectrum with increasing concentration (Figure 3). This is indicative of strong π–π stacking where protons on the periphery of the HBC core experience shielding effect from the aromatic ring of the adjacent HBC molecule. In addition, it was observed that the protons on the fluorene unit did not shift significantly with concentration. This suggests that only the HBC cores are in close proximity to each other in the aggregates with the bulky fluorene units arranged further apart. The ^{1}H NMR of hexakis-substituted FHBC **1** did not show any concentration dependence. Perhaps the steric bulk of the six fluorene units are preventing π–π stacking of the HBC cores.

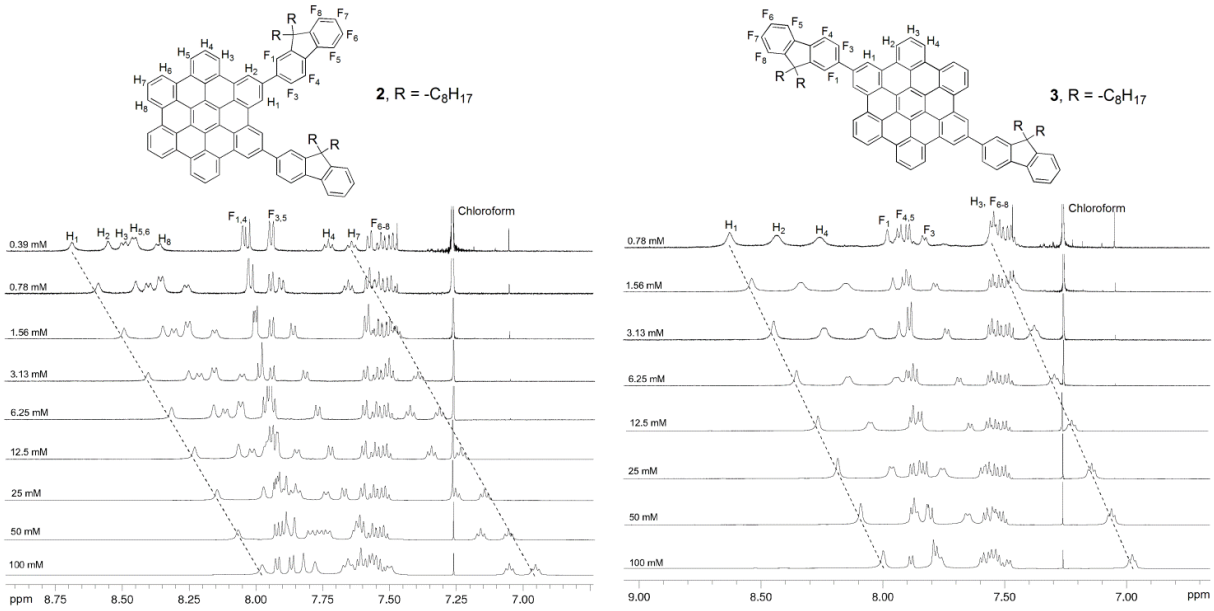

Figure 3. Illustration of changes in the ^{1}H NMR spectrum of FHBC compounds **2** and **3** by varying solution concentration ($CDCl_3$).

Ordered molecular aggregates of FHBC compounds **2** and **3** were also observed in solid state (Figure 4). Two-dimensional X-ray scattering (2D-WAXS) patterns were obtained from extruded filaments of FHBC compounds (Figure 5).[10] Clear meridional and equatorial scattering peaks were observed for compounds **2** and **3** (Figure 4b and 4c). The π–π stacking distance can be calculated from meridional scattering peaks while the equatorial peaks provided information on longer range order (Figure 5). Both compounds **2** and **3** showed columnar stacking with hexagonal packing of the columns (Figure 4b and 4c). Macroscopic domains of the columnar aggregates were also aligned in the direction of the extrusion (Figure 5). In line with the solution NMR data, the 2D-WAXS pattern of FHBC compound **1** did not show any meridional scattering (Figure 4a). Tapping mode atomic force microscopy (AFM) topography images showed micro-crystalline films for compounds **2** and **3** (Figure 4e and 4f). Upon thermal annealing (150 °C, 30 min), the crystalline domains were observably enlarged (Figure 4h and 4i). Again, a very smooth surface was observed for the bulky compound **1** in AFM indicating a lack of molecular order (Figure 4d). Further functionalization of FHBC compounds can also affect the way FHBC molecules aggregate in solution and in solid state.[9, 12-14] Figure 5 shows the 2D-WAXS patterns of FHBC-thiophene derivatives. Helical packing of FHBC-thiophene compound **23b** was observed presumably as a result of the steric bulk of the thiophene substituent forcing the molecules to π–π stack in a staggered manner (Figure 5). As the thiophene dendron becomes larger as in the case of compound **23c** and **23d**, lamella packing was preferred.[9] Similar trends in aggregation were recorded in other FHBC derivatives including the porphyrin and fullerene hybrids **24** and **25**. As these materials with the exception of FHBC-fullerene compound **25** are designed to be electron donor materials in bulk heterojunction (BHJ) solar cells, it was also important to examine the

solid state bulk structure of blend films with fullerene electron acceptor $PC_{61}BM$ (Figure 6). Tapping mode AFM topography images of blend films of FHBC **3** and $PC_{61}BM$ (1:2) revealed nano-scale phase separation of the donor and acceptor domains in as-casted samples (Figure 6a). Upon annealing at 150 °C for 15 s, the phase separated domains became larger (Figure 6b) and the corresponding thin film X-ray diffraction pattern showed hexagonally packed columnar structures (Figure 6c). The thermal annealing allowed the growth of larger ordered domains of FHBC compound **3**. This annealing step has dramatic effects on the BHJ solar cell performance (*vide infra*).

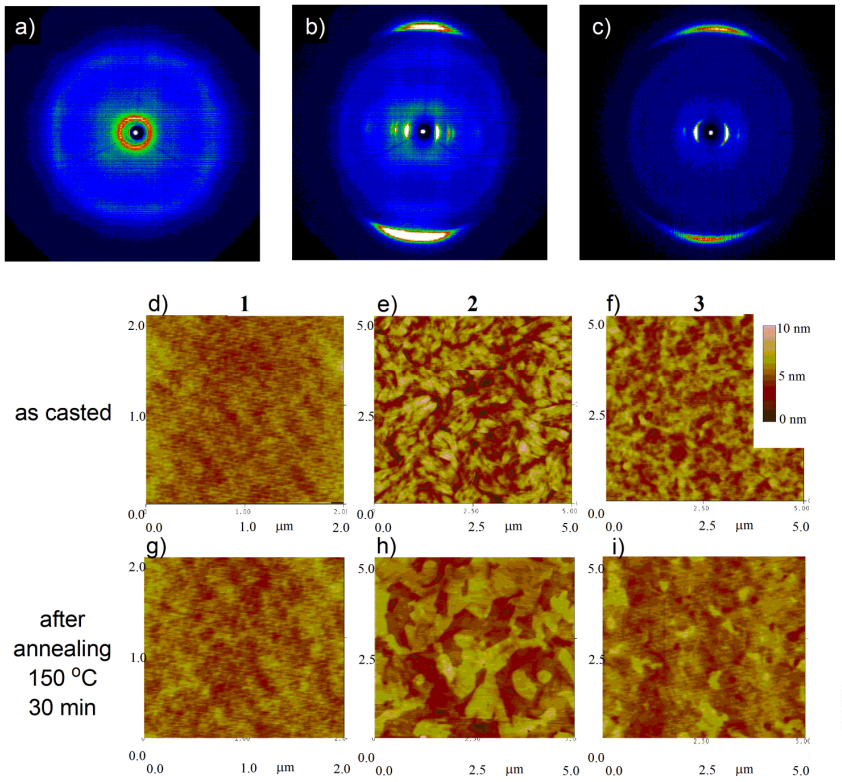

Figure 4. Two-dimensional wide-angle X-ray scattering (2D-WAXS) patterns and tapping mode atomic force microscopy (AFM) topography images for FHBC compounds (a, d, g) **1**, (b, e, h) **2** and (c, f, i) **3**.

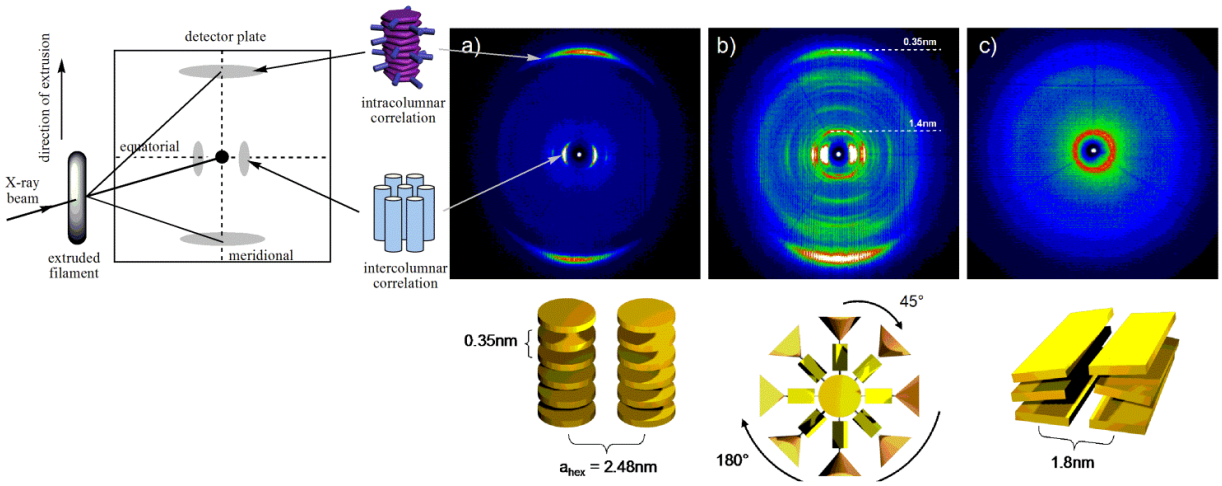

Figure 5. Two-dimensional wide-angle X-ray scattering (2D-WAXS) patterns of FHBC compounds (a) **3**, (b) **23b** and (c) **23c**.

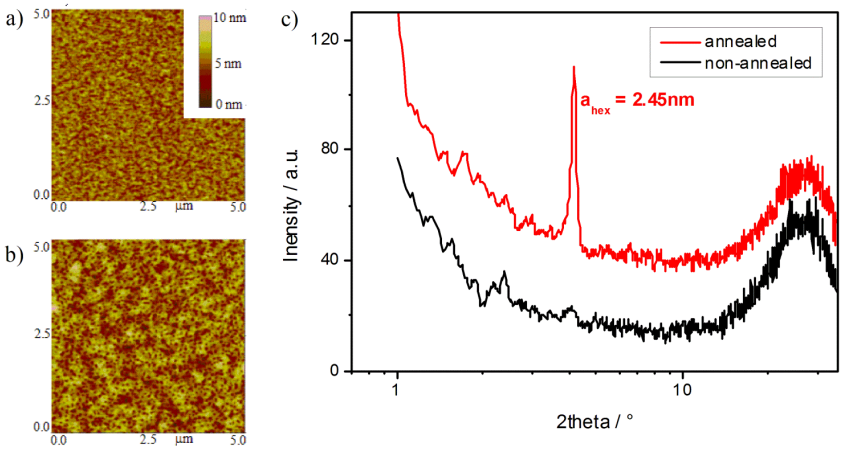

Figure 6. Tapping mode atomic force microscopy (AFM) topographic images of blend films containing FHBC **3** and $PC_{61}BM$ (a) before and (b) after annealing at 150 °C for 15 s. (c) Thin film X-ray diffraction of the blend films showing a diffraction peak indicative of ordered FHBC structures.

4. ORGANIC PHOTOVOLTAIC DEVICES

As mentioned in the previous section, the primary application of the FHBC materials is in BHJ solar cell devices.[9, 10, 12-14] A typical BHJ device structure is shown in Figure 7a. The transparent electrode is indium tin oxide (ITO) on glass. A layer of conducting polymer (PEDOT:PSS) is spin coated on top of the ITO to act as an electron blocking and surface smoothing layer. The active layer consisting of a blend of electron donor and acceptor materials is then deposited on the PEDOT:PSS. To complete the device, a metal top contact is usually deposited under vacuum. In some devices, an additional hole blocking layer is inserted between the active layer and the metal contact. This can be calcium, lithium fluoride or titanium oxide (Figure 7a). To assess the performance of devices, current-voltage characteristics are recorded in the dark and under solar simulated illumination. The current-voltage curves of BHJ device containing FHBC compound **3** and $PC_{61}BM$ (1:2) under illumination (AM 1.5G) before and after annealing are shown in Figure 7b.[10] It is clear that thermal annealing made a significant enhancement in device performance. Interestingly, the device performance decreased if longer periods of thermal annealing were applied. This suggests that the control of active layer morphology is key to efficient BHJ devices. Table 1 summarizes the performance of solar cell devices containing various FHBC derivatives showing open circuit voltage (V_{oc}), short circuit current density (J_{sc}), fill factor and power conversion efficiency (PCE). One correlation is particularly clear in this data. Well ordered FHBC domains in devices is very important to device performance. Donor FHBC compound **1** performed very poorly in devices (Table 1, entry i). This is directly related to the lack of molecular order in films containing compound **1** (Figure 4). This is in contrast to FHBC compounds **2** and **3** (Table 1, entry ii & iii). Another factor influencing device performance is the light absorption of the materials. For the FHBC-thiophene hybrid compounds **23a-d**, their increased absorptivity led directly to enhancement in photocurrent generation in the devices (Table 1, entry v-viii).[12] The use of the C_{70} fullerene derivative ($PC_{71}BM$) also increased the light absorbed by the active layer translating to higher currents. It is interesting to note that while the FHBC-porphyrin compound **24** has significantly enhanced absorption as a result of the porphyrin unit, the corresponding BHJ device performance was not as higher as expected (Table 1, entry ix).[13] This is a result of the bulky porphyrin groups adversely affecting the morphology of the active layer in devices. Even though the films can absorb large amount of light, the efficiency of charge separation and charge transport in these materials is relatively low. Lastly, it is also possible to design materials for single component solar cell devices. FHBC-fullerene compounds **25a** and **25b** contain electron donor and acceptor units in one molecule (Scheme 2).[14] This means these compounds can be used in the active layer of devices without blending of components. Single active component devices are simple to construct and the morphology of the active layer can be directly controlled by variation in molecular structure. While the performance of devices containing FHBC-fullerene **25a** was moderate, the potential is there for improvement (Table 1, entry x). The low photocurrent generated from the device indicated strong charge recombination in the active layer. It is thought that the donor and acceptor domains are too small for efficient charge transport to the electrodes.

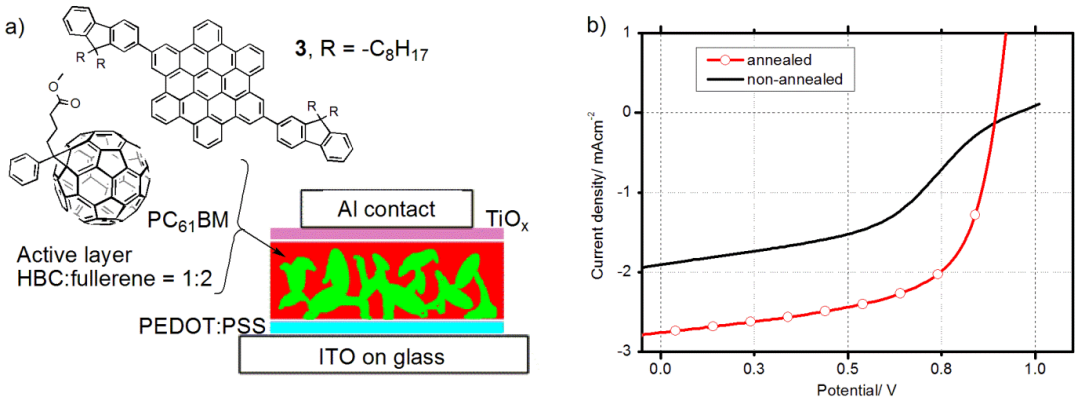

Figure 7. (a) Solar cell device structure and (b) current-voltage curve for solar cell device containing FHBC **3** and $PC_{61}BM$ (1:2) before and after annealing at 150 °C for 15 s.

Table 1. Device performance for solar cell devices containing various FHBC derivatives.

Entry	Donor	Acceptor	V_{oc} (V)	J_{sc} (mA/cm^2)	Fill factor	PCE %
i	**1**	$PC_{61}BM$	0.61	0.17	0.32	0.03
ii	**2**	$PC_{61}BM$	0.87	2.03	0.60	1.06
iii	**3**	$PC_{61}BM$	0.90	2.68	0.61	1.46
iv	**22**	$PC_{61}BM$	0.64	0.68	0.30	0.13
v	**23a**	$PC_{71}BM$	0.99	5.78	0.43	2.41
vi	**23b**	$PC_{71}BM$	1.02	5.46	0.42	2.35
vii	**23c**	$PC_{71}BM$	1.04	5.71	0.44	2.64
viii	**23d**	$PC_{71}BM$	1.00	5.41	0.41	2.27
ix	**24**[(a)]	$PC_{61}BM$	0.94	2.94	0.44	1.20
x	**25a**[(b)]	none	0.90	0.80	0.21	0.15
xi	**26**	$PC_{71}BM$	0.96	5.07	0.34	1.64

(a) Compound **24** was used in a ternary blend with compound **3** and $PC_{61}BM$. (b) Single component active layer containing compound **25a** only.

5. CONCLUSIONS

Over the past 3 years, we have developed a new class of fluorene substituted hexa-*peri*-hexabenzocoronene derivatives which showed great promise in solar cell applications. These compounds are not only solution processable but can also be easily functionalized which enables tuning of their properties. Despite the bulky 9,9-dioctylfluorene units, the majority of FHBC derivatives showed strong aggregation in solution and in solid state leading to long range ordered structures. As a consequence, FHBC materials have good charge transport properties. In devices containing blends of FHBC compounds and fullerene acceptors, ordered columnar structures are maintained in the active layer and good device performance was recorded. High power conversion efficiency of almost 3% was reported for FHBC-thiophene materials. In order to make further improvements on device performance, materials with high light absorptivity as well as good charge transport behavior have to be targeted.

[1] W. Pisula, X. Feng, and K. Müllen, "Charge-Carrier Transporting Graphene-Type Molecules," Chem. Mater., 23(3), 554-567 (2011).

[2] J. Wu, W. Pisula, and K. Müllen, "Graphenes as potential material for electronics," Chem. Rev., 107(3), 718-747 (2007).

[3] E. Clar, and C. T. Ironside, “Hexabenzocoronene,” Proc. Chem. Soc., 150 (1958).
[4] J. Piris, W. Pisula, A. Tracz *et al.*, “Thermal switching of the optical anisotropy of a macroscopically aligned film of a discotic liquid crystal,” Liq. Cryst., 31(7), 993-996 (2004).
[5] W. Pisula, Z. Tomovic, C. Simpson *et al.*, “Relationship between Core Size, Side Chain Length, and the Supramolecular Organization of Polycyclic Aromatic Hydrocarbons,” Chem. Mater., 17(17), 4296-4303 (2005).
[6] X. Dou, W. Pisula, J. Wu *et al.*, “Reinforced self-assembly of hexa-peri-hexabenzocoronenes by hydrogen bonds: from microscopic aggregates to macroscopic fluorescent organogels,” Chem. Eur. J., 14(1), 240-249 (2008).
[7] W. Jin, Y. Yamamoto, T. Fukushima *et al.*, “Systematic studies on structural parameters for nanotubular assembly of hexa-peri-hexabenzocoronenes,” J. Am. Chem. Soc., 130(29), 9434-40 (2008).
[8] J. P. Hill, W. Jin, A. Kosaka *et al.*, “Self-assembled hexa-peri-hexabenzocoronene graphitic nanotube,” Science, 304(5676), 1481-1483 (2004).
[9] W. W. H. Wong, C.-Q. Ma, W. Pisula *et al.*, “Self-assembling thiophene dendrimers with a hex-*peri*-hexabenzocoronene core - synthesis, characterization and performance in bulk heterojunction solar cells,” Chem. Mater., 22, 457-466 (2010).
[10] W. W. H. Wong, T. B. Singh, D. Vak *et al.*, “Solution processable fluorenyl hexa-*peri*-hexabenzocoronenes in organic field effect transistors and solar cells,” Adv. Funct. Mater., 20(6), 927-938 (2010).
[11] W. W. H. Wong, D. J. Jones, C. Yan *et al.*, “Synthesis, Photophysical, and Device Properties of Novel Dendrimers Based on a Fluorene-Hexabenzocoronene (FHBC) Core,” Org. Lett., 11(4), 975-978 (2009).
[12] W. W. H. Wong, C.-Q. Ma, W. Pisula *et al.*, “Fluorenyl Hexa-peri-hexabenzocoronene-Dendritic Oligothiophene Hybrid Materials: Synthesis, Photophysical Properties, Self-Association Behaviour and Device Performance,” Chem. Eur. J., 17(20), 5549-5560 (2011).
[13] W. W. H. Wong, T. Khoury, D. Vak *et al.*, “A porphyrin-hexa-peri-hexabenzocoronene-porphyrin triad: synthesis, photophysical properties and performance in a photovoltaic device,” J. Mater. Chem., 20(33), 7005-7014 (2010).
[14] W. W. H. Wong, D. Vak, T. B. Singh *et al.*, “Ambipolar Hexa-peri-hexabenzocoronene-Fullerene Hybrid Materials,” Org. Lett., 12(21), 5000-5003 (2010).
[15] E. Clar, [Polycyclic Hydrocarbons: Their Synthesis and Reactions. Vol. 1], (1964).
[16] E. Clar, C. T. Ironside, and M. Zander, “28. The electronic interaction between benzenoid rings in condensed aromatic hydrocarbons. 1 : 12-2 : 3-4 : 5-6 : 7-8 : 9-10 : 11-hexabenzocoronene, 1 : 2-3 : 4-5 : 6-10 : 11-tetrabenzoanthanthrene, and 4 : 5-6 : 7-11 : 12-13 : 14-tetrabenzoperopyrene,” Journal of the Chemical Society (Resumed), 142-147 (1959).
[17] E. Clar, [Polycyclic Hydrocarbons. Vol. 2], (1964).
[18] J. C. Fetzer, [Large (C>=24) polycyclic Aromatic Hydrocarbons] John Wiley and Sons: New York, (2000).